Estimating Drone Motor Related Acoustic Transfer Function: A Preliminary Investigation

Wageesha Manamperi, Thushara D. Abhayapala, Jihui Zhang and Prasanga N. Samarasinghe
Research School of Electrical, Energy and Materials Engineering
College of Engineering and Computer Science
Australian National University
Canberra, Australia
E-mail: {*wageesha.manamperi, thushara.abhayapala, jihui.zhang, prasanga.samarasinghe*}@*anu.edu.au*

***Abstract*—The potential of drone based services is enormous with applications ranging from consumer product delivery to health services. When meeting this demand, one of the major challenges we face is the noise produced by drones, which not only contributes to listener discomfort, but also hinders the device's ability to effectively communicate via audio. Thus, there exists a pressing need for understanding the characteristics of drone related noise, which can then be suppressed using suitable methods. This paper presents a preliminary study on modeling the relationship between input motor current and acoustic noise produced by a drone. An experimental study is conducted indoors for a drone under hovering manoeuvre with a single active motor and propeller. The drone noise was measured by a single on-board microphone. We identify multiple tones or *harmonics* in the drone noise spectrum that vary proportionally to the motor current. Based on this observation, we define a transfer function between the input current and output noise, and model its harmonic behaviour using a higher order polynomial function. A detailed error analysis is presented to validate the model.**

I. Introduction

Unmanned aerial vehicles (UAVs) or drones are rapidly transforming and/or replacing many activities in the commercial, recreational and military spaces. For example, they have a lot of potential in consumer/health package delivery [1], emergency rescue missions [2], firefighting, surveillance [3], video capturing [4], [5], and wild-life management [6] etc. However, the widespread deployment of these applications is not yet accepted by the public due to two main reasons; (i) privacy concerns, and (ii) noise pollution. Addressing the latter is the motivation for this work.

Drones utilize multiple modalities for communication and information capture, where audio is of predominant importance. Thus, audio signal processing for drone applications has significant interest. While there exist a large amount of recent work on audio signal processing for drones ranging from source localization to signal classification [2], [7]–[11], the aforementioned challenge of drone related noise reduction is still very much an open problem. The majority of the noise around the drone is produced by itself. As such, there exist a great need to systematically understand and mitigate the noise emission by drones in order to enhance the user experience [12].

The acoustic spectrum of a typical drone is composed of tonal noise and broadband noise where tonal noise generates discrete tones characterized as *harmonics* whereas the broadband noise is due to turbulence and the airflow through the propeller blades [13]. It is identified that the main sources of drone noise is due to motors and propellers [14]. Several previous work have analysed drone noise sources such as motor [15] and propellers [16], [17] separately.

Many work related to drone noise analysis often also include the drone's ability to localize sound sources amidst noise [2], [7]–[11], [14]. In [7], a UAV-embedded dataset is presented with the rotational speed of propeller for different flight configurations, and the authors observed the relationship between the spectral harmonic components and motor speeds. In [11], the suppression of drone noise is addressed using template-based approaches that estimate the noise correlation matrix using speed data. There are many studies on aerodynamic performance analysis model for drone propeller [13], [18], but fewer on noise. Most of the previous work have presented drone noise analysis using free-field or ground-based microphone arrays [19], [20]. While such analysis using on-board microphones is rare, in [14], an embedded microphone array was used to model drone noise in terms of an equivalent source distribution plus a diffuse field. Although not directly performing drone noise analysis, some other loosely related work include machine learning based feature extraction and classification of drone noise for acoustic detection of UAVs [21]–[23], and passive drone noise reduction via propeller design optimization methods (lighter propeller, shroud design the use of ducts) [24].

The objective of this work is to present our preliminary work on deriving a drone related acoustic transfer function that can in return estimate the noise generated for a given flight manoeuvre. Our approach is to start from recorded drone noise, observe their most evident characteristics, and fit a mathematical model(s) to these characteristics. We use an on-board microphone to obtain noise when only a single motor and propeller pair is active while the drone is at a steady state of hovering manoeuvre, and we repeat the measurement for different motor currents. By analyzing the recorded noise spectrum for varying currents, our intention is to find a mathematical relationship between the input current and apparent characteristics of the said spectrum. The remainder of this paper is organized as follows. Section II defines the problem.

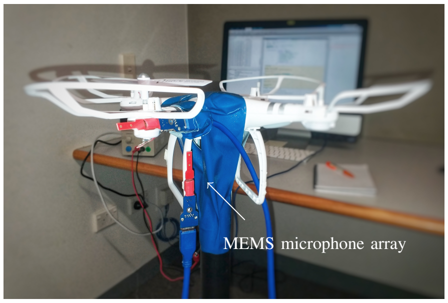

Fig. 1. A drone with microphone arrays attached to the body.

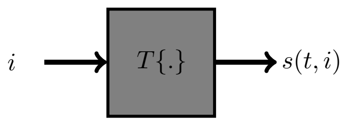

Fig. 2. 'Black Box' model; The transfer function: motor current, i as input signal whereas signal received by the microphone, $s(t, i)$ as the output signal to the system.

Section III describes the experimental setup with an analysis of the results. Section IV introduces the current to noise transfer function with a model to obtain the harmonic frequencies of drone motor noise. Section V presents the estimation of the model parameters and Section VI concludes the paper.

II. Problem Statement

We aim to analyze the relationship between the current that drives the motor and the resulting acoustic signal received from a microphone attached to the body of drone (as shown in Fig. 1). The drone motor is driven by an electronic speed controller such that it regulates the current through the motor to control the rotational speed of the rotor. Thus, drone noise may be modeled against the input current that drives the motor or the rotational speed of rotors, and we use the former.

Let's denote the current through the motor as i (constant over time for a fixed manoeuvre), and the noise signal received by the microphone at time t as $s(t, i)$. Then, the drone motor related acoustic transfer function can be modeled as 'Black Box' model as shown in Fig. 2, and can express as

$$s(t, i) = T\{t, i\}.$$

In this work, we aim to investigate the transfer function between the current through the motor and corresponding sound pressure measured from the microphone attached to the body of the drone, and also parameterise the transfer function for a fixed manoeuvre.

III. Experimental Analysis

In this section, we discuss the experimental setup, measurement results and its analysis. Note that drones can operate in different flight modes and manoeuvres by controlling the throttle, roll, pitch, and yaw. In the following, we consider a hovering maneuver where constant current passes through all the motors, which leads to operating them at the same angular speed.

Fig. 3. Experimental Setup, with microphone array attached to the body of drone closer to the selected motor.

A. Experimental Setup

Our objective is to find a relationship between the driving current i of the motor and the noise field captured by an on-board microphone. For this experiment, we drive a single motor using a known input current i and acquire the sound pressure signal $s(t, i)$ received by the microphone fixed to the under-body of the drone. We repeat the measurement over different currents within the operating range of the motor.

The experiment is carried out in a quiet room with dimensions of length 500 cm, width 410 cm and height 245 cm, and a room reverberation time of T_{60} of 140 ms. We mount the drone to a 1 m tall rigid stand to minimize vibrations and. Using a bench top power supply, we operate a single motor attached with a two-bladed propeller. The drone we use consists of clockwise and anti-clockwise propellers with a diameter of 150 mm, and they are driven by direct current brushed permanent magnet motors. Note that the concept set out in this work can be used to extend for the brushless direct current motor and brushless alternating current motor as well. The power supply is driven at Constant Current (CC) mode, for each measurement and repeated at 50 mA steps ranging from 100 mA to 1000 mA. At each step, the acoustic measurements are obtained for a duration of 10 seconds using a Micro-Electro-Mechanical System (MEMS) microphone and a USB-powered external audio interface with 48KHz sampling frequency. The microphone was attached to the landing gear of the drone, close to the motor (as shown in Fig. 3).

B. Analysis of Results

In this subsection, we present the recorded data for varying input motor currents, and draw insights in to their apparent characteristics.

Figure 4 shows the frequency spectrum of noise recorded by the microphone when only one of the motors is driven by an input current of (i) 100 mA (black), and (ii) 1000 mA (blue). Note that, a low-pass filter was used to remove frequencies over 10 kHz. Also, shown in red is the spectrum

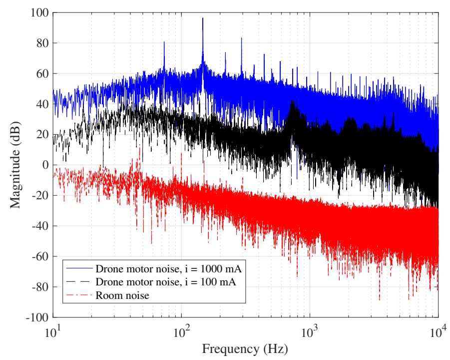

Fig. 4. Frequency spectrum of the recorded drone motor noise at 1000 mA and 100 mA with background noise.

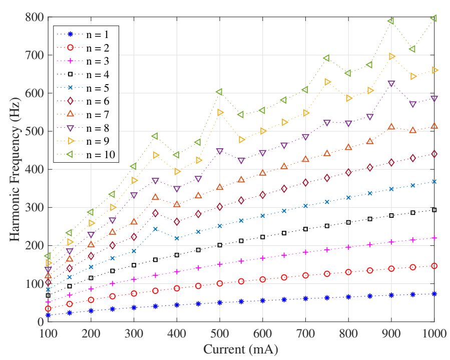

Fig. 5. Harmonic frequency with respect to motor current.

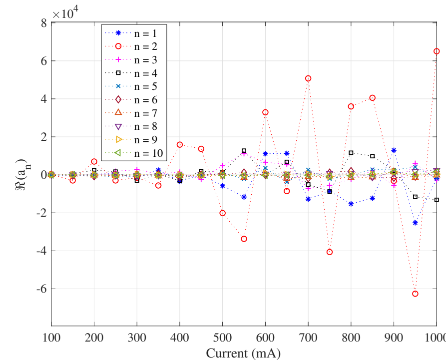

Fig. 6. Real part of the harmonics amplitude, $\Re(a_n)$ with respect to motor current, i.

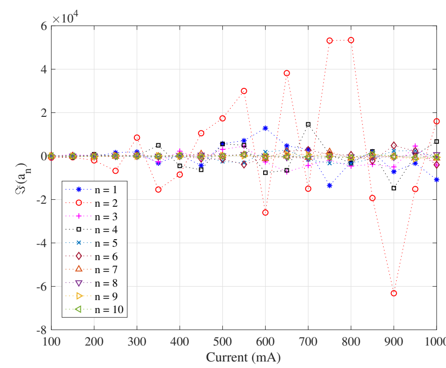

Fig. 7. Imaginary part of the harmonics amplitude, $\Im(a_n)$ with respect to motor current, i.

of background noise measured by the microphone when the drone was inactive. Note that the background room noise is negligible compared to drone noise. However, we subtract room noise from the acoustic measurements in spectral domain for normalization. From Fig. 4, we can observe a number of peaks in the noise spectrum reflecting multiple tones. We refer to these distinct tones as *harmonics*, because they are almost harmonically related.

Figure 5 shows how the variation of first 10 *harmonics* ω_n, $n = 1, \dots, 10$ as a function of the driving current i of the drone motor. Figures 6 and 7 plot the real and imaginary parts of the amplitude of each of the first 10 dominant harmonics, respectively. We can observe that there is a certain pattern in the above curves, inferring to an underlying relationship between the amplitude and frequencies of the harmonics and the driving current of the motor.

In the next section, we will model the experimental results to identify the complex relationship between the noise field harmonics and the motor current.

IV. Current to Noise Transfer Function

In this section, we obtain an expression for the current to noise transfer function, considering only the significant *harmonics* of the received signal.

Let N be the number of harmonics, then the received signal can be given by

$$s(t,i) = \sum_{n=-N, n\neq 0}^{N} a_n(i)\, e^{j\omega_n(i)t}, \tag{1}$$

where $\omega_n(i)$ is the n^{th} harmonic frequency and $a_n(i)$ is the amplitude of the n^{th} harmonic. Note that

$$\omega_{-n} = -\omega_n,$$

$s(t,i)$ is a real signal, and $a_n(i)$ is a complex amplitude with the property,

$$a_{-n} = a_{n^*}.$$

Figures 6 and 7 illustrate that real and imaginary parts of a_n grow exponentially with current. Figure 5 depicts the behaviour of harmonic frequency against input motor current. We observe that harmonic frequencies, w_n seem to behave as a higher order polynomial of current i. Hence, we may be able to model $w_n(i)$ as

$$\omega_n(i) = \sum_{m=0}^{M} p_{nm}\, i^m, \tag{2}$$

where M is the order of the polynomial, m is the index and p_{nm} are the coefficients of the polynomial. We aim to estimate

p_{nm} to show the relationship between the drone motor driving current and the harmonics of the noise. In this work, we leave out the modelling of a_n and hope to address it in a future publication.

V. Parameter Estimation

Here, we provide a way to estimate the proposed model parameters $p_{nm} \in \mathbb{R}$ in (2) using a least-squares approximation method that minimizes the squared error. We evaluate the model accuracy based on the mean squared error (MSE).

Suppose we have Q samples $\{(i_q, \omega_n(i_q))\}_{q=1}^{Q}$ where $i_q, \omega_n(i_q) \in \mathbb{R}$. We modify model (2) as

$$\omega_n(i_q) = \sum_{m=0}^{M} p_{nm}\, i_q^m + \epsilon_q,$$

where ϵ_q is the random error component of the q^{th} case. This can be written in matrix form as

$$\begin{bmatrix} \omega_n(i_1) \\ \omega_n(i_2) \\ \vdots \\ \omega_n(i_Q) \end{bmatrix} = \begin{bmatrix} 1 & i_1 & i_1^2 & \dots & i_1^M \\ 1 & i_2 & i_2^2 & \dots & i_2^M \\ \vdots & \vdots & \vdots & \ddots & \vdots \\ 1 & i_Q & i_Q^2 & \dots & i_Q^M \end{bmatrix} \begin{bmatrix} p_{n0} \\ p_{n1} \\ \vdots \\ p_{nM} \end{bmatrix} + \begin{bmatrix} \epsilon_1 \\ \epsilon_2 \\ \vdots \\ \epsilon_M \end{bmatrix},$$

$$\omega_\mathbf{n} = \mathbf{X}\ \mathbf{p_n} + \epsilon,$$

where the vector $\omega_\mathbf{n} \in \mathbb{R}^Q$ and the matrix $\mathbf{X} \in \mathbb{R}^{Q\times(M+1)}$ are the given data, and $\mathbf{p_n} \in \mathbb{R}^{(M+1)}$ is the unknown parameter vector. With $Q \geq (M+1)$, the basic least-squares approximation method [25] involves estimating $\mathbf{p_n}$, as a solution of the optimization problem such that squared error is minimized.

$$\hat{\mathbf{p}}_\mathbf{n} = \underset{\mathbf{p_n}\in\mathbb{R}}{\operatorname{argmin}} ||\mathbf{X}\ \mathbf{p_n} - \omega_\mathbf{n}||^2. \tag{3}$$

The least-squares approximation solution to (3) is

$$\hat{\mathbf{p}}_\mathbf{n} = (\mathbf{X}^T\mathbf{X})^{-1}\mathbf{X}^T\omega_\mathbf{n},$$

where $\hat{\mathbf{p}}_\mathbf{n}$ is an unbiased estimator of $\mathbf{p_n}$. While the above can be computed via singular value decomposition, for the purpose of this paper, we use a simple least-squares method to fit the data resulting in a model function given by

$$\hat{\omega}_\mathbf{n} = \mathbf{X}\hat{\mathbf{p}}_\mathbf{n}.$$

Based on (3), the best estimate of the model $\hat{\mathbf{p}}_\mathbf{n}$ can be obtained by minimizing the MSE given by

$$\text{MSE} = \frac{1}{Q}\sum_{q=1}^{Q}(\omega_\mathbf{n} - \hat{\omega}_\mathbf{n})^2.$$

Figure 8 presents the results after fitting an M^{th} order polynomial where $M \in [3, 4, \dots, 8]$. From Fig. 8(a) we observe that MSE decreases more rapidly with increasing M for $n \in [1, 2, \dots, 4]$. From Fig. 8(b), we observe that MSE estimators are comparably high and become stable with M for $n \in [5, 6, \dots, 10]$. This may be due to the notches appearing in Fig. 5. The reason for these notches is not clear at this stage.

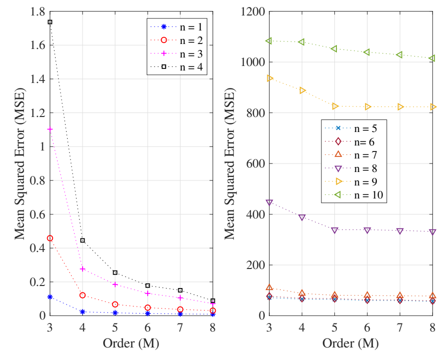

Fig. 8. MSE estimator of $\hat{\omega}_\mathbf{n}$ for $n \in [1, 2, \dots, 10]$ with repect to the order of the polynomial M.

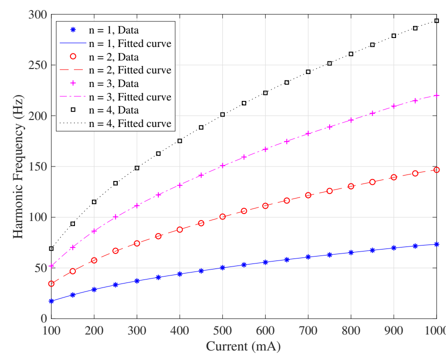

Fig. 9. Harmonics frequency, ω_n, $n = 1, \dots, 4$ mapped with the motor current, i. Markers are actual data whereas lines are polynomial fit.

It can be due to a measurement error or due to the resonance effect in the room.

From the above observation, we decide to fit a seventh order $M = 7$ polynomial regression model for the *harmonic* frequency variation over current. Figure 9 shows the reconstructed harmonics using the above model for the first four *harmonics*. We observe that the seventh-degree polynomial provides a good approximation for ω_n, where $n = 1, \dots, 4$ with respect to the measured value. In Fig. 10 we show similar results for higher order harmonics from $n \in [5, 6, \dots, 10]$, which still manage to achieve 95% confidence interval estimates. These results confirm that the harmonic frequencies of drone motor noise against input current can be successfully modeled using higher order polynomials.

VI. Conclusions

In this paper, we presented measurement data and analysis of acoustic noise produced by a commercial drone at steady state of hovering. Motivated by an apparent harmonic structure observed in the noise measurements, we defined a transfer function between the motor current and the drone noise. The frequency behaviour of these harmonics were modeled using higher order polynomials, and we provided a detailed error

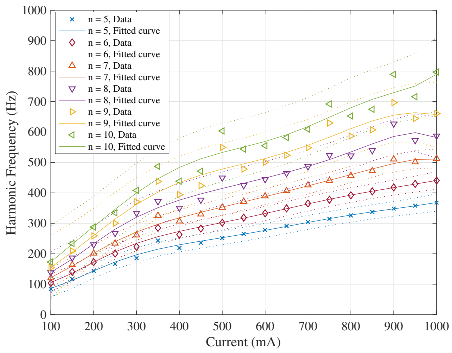

Fig. 10. Harmonics frequency, ω_n, $n = 5, \ldots, 10$ mapped with the motor current, i. Markers are actual data whereas lines are polynomial fit and dotted lines are 95% confidence interval.

analysis validating the model accuracy. In future work, we hope to derive another model for harmonic strength behaviour against frequency, which appear to have a negatively un-damped sinusoidal structure.

References

[1] S. M. Shavarani, M. G. Nejad, F. Rismanchian, and G. Izbirak, "Application of hierarchical facility location problem for optimization of a drone delivery system: a case study of Amazon prime air in the city of San Francisco," *Int. J. of Adv. Manuf. Technol.*, vol. 95, no. 9 - 12, pp. 3141 – 3153, 2018.

[2] M. Basiri, F. Schill, P. U. Lima, and D. Floreano, "Robust acoustic source localization of emergency signals from micro air vehicles," in *Proc. IEEE/RSJ Int. Conf. on Intell. Robots Syst.*, Oct. 2012, pp. 4737 – 4742.

[3] H. E. de Bree, "Acoustic vector sensors increasing UAV's situational awareness," SAE Technical Paper, Tech. Rep. 0148 - 7191, 2009.

[4] L. Meier, P. Tanskanen, F. Fraundorfer, and M. Pollefeys, "Pixhawk: A system for autonomous flight using onboard computer vision," in *Proc. IEEE Int. Conf. on Robot. Automat.*, May 2011, pp. 2992 – 2997.

[5] D. Floreano and R. J. Wood, "Science, technology and the future of small autonomous drones," *Nature*, vol. 521, no. 7553, pp. 460 – 466, 2015.

[6] J. C. Hodgson, S. M. Baylis, R. Mott, A. Herrod, and R. H. Clarke, "Precision wildlife monitoring using unmanned aerial vehicles," *Sci. Rep.*, vol. 6, no. 1, p. 22574, 2016.

[7] M. Strauss, P. Mordel, V. Miguet, and A. Deleforge, "DREGON: Dataset and methods for UAV-embedded sound source localization," in *Proc. IEEE/RSJ Int. Conf. on Intell. Robots Syst.*, Oct. 2018, pp. 1 – 8.

[8] K. Hoshiba, K. Washizaki, M. Wakabayashi, T. Ishiki, M. Kumon, Y. Bando, D. Gabriel, K. Nakadai, and H. G. Okuno, "Design of UAV-embedded microphone array system for sound source localization in outdoor environments," *Sensors*, vol. 17, no. 11, p. 2535, 2017.

[9] T. Ohata, K. Nakamura, T. Mizumoto, T. Taiki, and K. Nakadai, "Improvement in outdoor sound source detection using a quadrotor-embedded microphone array," in *Proc. IEEE/RSJ Int. Conf. on Intell. Robots Syst.*, Sep. 2014, pp. 1902 – 1907.

[10] K. Okutani, T. Yoshida, K. Nakamura, and K. Nakadai, "Outdoor auditory scene analysis using a moving microphone array embedded in a quadrocopter," in *Proc. IEEE/RSJ Int. Conf. on Intell. Robots Syst.*, 2012, pp. 3288 – 3293.

[11] K. Furukawa, K. Okutani, K. Nagira, T. Otsuka, K. Itoyama, K. Nakadai, and H. G. Okuno, "Noise correlation matrix estimation for improving sound source localization by multirotor UAV," in *Proc. IEEE/RSJ Int. Conf. on Intell. Robots Syst.*, 2013, pp. 3943 – 3948.

[12] A. W. Christian and R. Cabell, "Initial investigation into the psychoacoustic properties of small unmanned aerial system noise," in *Proc. AIAA/CEAS Aeroacoustics Conf.*, 2017, p. 4051.

[13] K. S. Brentner and F. Farassat, "Modeling aerodynamically generated sound of helicopter rotors," *Progress in Aerospace Sciences*, vol. 39, no. 2 - 3, pp. 83 – 120, Feb. 2003.

[14] L. Wang and A. Cavallaro, "Ear in the sky: ego-noise reduction for auditory micro aerial vehicles," in *Proc. IEEE Int. Conf. on Adv. Video and Signal Based Surveillance*, 2016, pp. 152 – 158.

[15] D. L. Huff and B. S. Henderson, "Electric motor noise for small quadcopters: Part 1–acoustic measurements," in *Proc. AIAA/CEAS Aeroacoustics Conf.*, 2018, p. 2952.

[16] G. Sinibaldi and L. Marino, "Experimental analysis on the noise of propellers for small UAV," *Applied Acoustics*, vol. 74, no. 1, pp. 79 – 88, Jan. 2013.

[17] S. O. Afari, *Prediction of Noise Associated with an Isolated UAV Propeller*. M.S. thesis, Dept. Aerosp. Eng., Embry-Riddle Aeronautical Univ., Daytona Beach, Florida, 2019, [Online]. Available: https://commons.erau.edu/cgi/viewcontent.cgi?article=1463&context=edt.

[18] W. A. Anemaat, M. Schuurman, W. Liu, and A. A. Karwas, "Aerodynamic design, analysis and testing of propellers for small unmanned aerial vehicles," in *Proc. AIAA Aerospace Sciences Meeting*, 2017, p. 0721.

[19] T. Zhou, H. Jiang, Y. Sun, R. J. Fattah, X. Zhang, B. Huang, and L. Cheng, "Acoustic characteristics of a quad-copter under realistic flight conditions," in *Proc. AIAA/CEAS Aeroacoustics Conf.*, 2019, p. 2587.

[20] J. A. Feight, S. Whyte, J. D. Jacob, and R. J. Gaeta, "Acoustic characterization of a multi-rotor UAS as a first step towards noise reduction," in *Proc. AIAA Aerospace Sciences Meeting*, 2017, p. 1174.

[21] S. Al-Emadi, A. Al-Ali, A. Mohammad, and A. Al-Ali, "Audio based drone detection and identification using deep learning," in *Proc. Int. Wireless Commun. & Mobile Comput. Conf.*, Jun. 2019, pp. 459 – 464.

[22] A. Bernardini, F. Mangiatordi, E. Pallotti, and L. Capodiferro, "Drone detection by acoustic signature identification," *Electronic Imaging*, no. 10, pp. 60 – 64, 2017.

[23] A. A. Cabrera-Ponce, J. Martinez-Carranza, and C. Rascon, "Detection of nearby UAVs using CNN and Spectrograms," in *Proc. Int. Micro Air Vehicle Conf. and Competition*, Oct. 2019.

[24] Z. Lu, M. Debiasi, and B. C. Khoo, "Acoustic characteristics of a multirotor MAV and its noise reduction technology," in *INTER-NOISE and NOISE-CON Congr. and Conf. Proc.*, vol. 253, Aug. 2016, pp. 393 – 403.

[25] C. L. Lawson and R. J. Hanson, *Solving least squares problems*. Society for Industrial and Applied Mathematics, Jan. 1995.